A DFT study on the effect of metal, anion charge, heteroatom and structure upon the relative basicities of polyoxoanions

Jorge A. Fernández [a], Xavier López [b], Josep M. Poblet [a],*

[a] *Departament de Química Física i Inorgànica, Universitat Rovira i Virgili, Marcel·lí Domingo s/n, 43007 Tarragona, Spain*
[b] *Laboratoire de Chimie Quantique, UMR 7551, CNRS and Université Louis Pasteur, 4 rue Blaise Pascal, F-67000 Strasbourg, France*

Available online 26 August 2006

Abstract

In many reactions catalyzed by polyoxoanions, the first step involves attaching a proton at the anion so that the activated species can react with the substrate. The present study focuses on this first step and makes a detailed analysis of the factors that affect the basicity of the distinct oxygen sites in a polyoxometalate. Several prototypical polyoxoanions were studied in solution using the conductor-like screening model (COSMO) to model the solution. The nucleophilicity of a given site depends mainly on the coordination type, the metal to which the oxygen is linked, the charge of the anion and the bonding angle in the bridging oxygen sites. The coordinated metal and the coordination type are the most important. We discuss in detail the effect of the charge and of the charge density of the anion on the basicity of the polyoxoanion.
© 2006 Elsevier B.V. All rights reserved.

Keywords: COSMO; Polyoxometalates (POMs); Polyoxoanion

1. Introduction

The applications of polyoxometalates (POMs) [1] have been studied in many fields from medicine to materials [2,3] for several decades now. The physicochemical properties of these molecular metal-oxide systems are mostly a function of the nature and oxidation state of the metal atoms that make up the frameworks. Typically, these frameworks consist of Mo or W in their highest oxidation states, and Nb, V or Ti atoms are also incorporated into many POM structures to customize or tune their properties [4,5]. The chemical properties of POMs are also affected by their structure. The most common classification of POMs divides them into two groups: (1) isopolyanions (IPAs), which have only one structural type of metal atom with the general formula $M_mO_y^{q-}$, and (2) heteropolyanions (HPAs), with the formula $X_rM_mO_y^{q-}$, where X is the so-called internal atom or *heteroatom* [1]. Despite this classification, the main properties are similar for all POMs, and they can be rationalized by taking into account the same principles. Nevertheless, their chemical and structural properties, which are responsible for their highly oxidizing nature and strong acidity in solution, are extremely singular. The reason for their strong acidity in solution is that their surface charge density is very low [6], which means that many of them, despite their anionic nature, exist in solution as non-protonated species at relatively low pH [7]. Some previous reports have dealt with the importance of HPAs as strong acid catalysts in both solid state and in solution [8].

POMs feature some exceptional characteristics to be catalysts, like the reversible redox chemistry at low potential, the high hydrolytic stability or the fast reoxidation by O_2 in both aqueous and non-aqueous media. Generally, reactions catalyzed by heteropolyanions can be considered in two ways. The strong acidity of POMs, often 100–1000 times higher than that of sulfuric acid, makes it possible to carry out the catalytic process at lower acid concentrations and to recover the catalyst from the homogeneous reaction mixture more easily. In many catalytic reactions involving POMs, attachment of a proton at the catalytic center is the starting point. Interestingly, the catalytic activity of POMs usually parallels their acid strength. Therefore, from this point of view, these reactions may be represented by the conventional mechanism of Brønsted-acid catalysis. In addition, the possibility of substituting metal atoms in the addenda framework makes it possible to tune the redox and acid–base properties of POMs. As a matter of fact, the incorporation of more electronegative atoms into the cluster leads to the appearance of new reactive sites.

* Corresponding author.
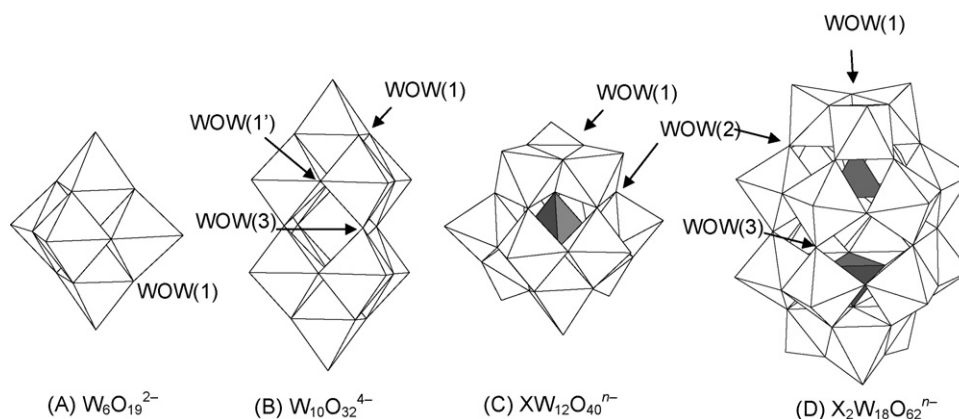 *E-mail address:* josepmaria.poblet@urv.net (J.M. Poblet).

Fig. 1. Polyhedral view of (A) Lindqvist, (B) decatungstate, (C) Keggin and (D) Dawson anions. Octahedra represent WO_6 units, with oxygens located at the vertices. Positions labeled W–O–W(1–3) are the bridging oxygen types present in such frameworks. See text for details.

The ability to attach or release protons in POMs has been investigated in the past but, nowadays, systematic knowledge of the factors that affect the protonation of POMs is still needed. We are not aware of any systematic study on the relationship between acid–base properties and chemical composition. At most, a few theoretical studies have computed the protonation energies (PE) of some polyoxoanions [9]. This paper does not aim to predict or to reproduce the exact protonation energies of POMs, but to establish how certain factors affect their basicity. Among other things, we shall discuss the importance of chemical composition, protonation site and anion charge.

2. Computational details

We computed all the molecules discussed here with the ADF 2003.01 [10] implementation of the density-functional theory. The calculations are characterized by the local density approximation featuring the $X\alpha$ model for exchange with Becke's gradient-corrected functional [11], and the VWN parameterization for correlation [12] corrected with Perdew's functional [13]. The basis functions for describing the valence electrons of all the atoms are Slater-type orbitals of triple-ζ + polarization quality. The internal or *core* electrons (O: 1s; P, Si, Al: 1s–2s; Ti, V: 1s–2p; Nb, Mo: 1s–3d; Ta, W: 1s–4d) were frozen. We applied scalar relativistic corrections to them – *zeroth-order regular approximation* (ZORA) – via the core potentials generated with the program DIRAC [10]. The structures of all clusters discussed here were fully optimized in the presence of a model solvent, accounted for by applying the *conductor-like screening model* (COSMO) [14] implemented as part of the ADF code [15]. To define the cavity surrounding the molecules, we used the solvent-excluding-surface method and a pruned tesserae. To obtain the electron density in solution, we first let the SCF converge without solvent effects and, thereafter, the COSMO was turned on to include the solvent effects variationally. The ionic radii for the POM atoms, which actually define the size of the solvent cavity where the target molecule remains, were chosen to be 0.74 Å for all metal ions except V^V, to which we chose 0.68, 1.20 Å for H and 1.52 Å for O^{2-}. The dielectric constant

was set equal to 78.4 for modeling water. All non-protonated and protonated anions were fully optimized in solution.

3. Results and discussion

We computed the total binding energies for protonated and non-protonated POM anions, as well as for H_2O and H_3O^+. The protonation energies discussed are associated to the following general process:

$$POM^{q-} + H_3O^+ \rightarrow H\text{-}POM^{(q-1)-} + H_2O$$
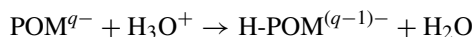
All the energies discussed in this section are arbitrarily referred to the PE of $W_6O_{19}^{2-}$ at the W–O–W site, to which we assign a value of zero in order to remove the main source of error in this study, which is the calculation of the solvation energies associated to H_3O^+ and H_2O. The results are split into two main subsections: the first discusses single-addenda $W_6O_{19}^{2-}$, $XW_{12}O_{40}^{q-}$ (X = P^V, Si^{IV}, Al^{III} and q = 3, 4, 5), $W_{10}O_{32}^{4-}$ and $P_2W_{18}O_{62}^{6-}$ polytungstates, and the second analyzes some mixed-addenda derivatives of the Lindqvist and Keggin anions, namely, $W_{6-x}M_xO_{19}^{n-}$ and $XW_{12-x}M_xO_{40}^{n-}$, with the same X and M = V^V, Nb^V and Ti^{IV} [16]. The geometrical parameters obtained from DFT calculations are, in general, in excellent agreement with the experimental values. The optimization of the structures including the solvation always improves the geometries [17] and only the M=O distances are systematically computed to be slightly longer than the experimental ones (0.01–0.07 Å), depending on the anion charge.

3.1. Single-addenda compounds

This series of anions contains the Lindqvist, Keggin decatungstate and Dawson polytungstates (see Fig. 1 for polyhedral views and oxygen labeling). There are four types of bridging W–O–W oxygen sites: in types (1) and (1′) the oxo ligand links two edge-sharing octahedra; in type (2) the oxygen links two corner-sharing octahedra; and finally type (3) is also a corner-sharing bridging oxygen with a larger bonding angle and located in the belt region in decatungstate and

Table 1
Computed protonation energies at different oxygen sites for Lindqvist, Keggin, Decatungstate and Dawson anions[a]

	WOW(1)	WOW(1′)	WOW(2)	WOW(3)	W=O
$W_6O_{19}^{2-}$	0.0	–	–	–	+7.6
$W_{10}O_{32}^{4-}$ [b]	−8.4	−2.5	–	+1.1	+2.3
$PW_{12}O_{40}^{3-}$	+4.4	–	+4.9	–	+12.2
$SiW_{12}O_{40}^{4-}$	−0.2	–	+2.5	–	+9.4
$AlW_{12}O_{40}^{5-}$	−5.6	–	−4.6	–	+3.9
$P_2W_{18}O_{62}^{6-}$	−6.2	–	−4.5	−2.0	−0.6

[a] The energies (in kcal mol^{-1}) are relative to protonation at W–O–W in $W_6O_{19}^{2-}$.
[b] Two different W–O–W(1) sites are given for $W_{10}O_{32}^{4-}$, the most negative corresponds to W–O–W(1) and the less to W–O–W(1′) in Fig. 1.

Dawson anions. Distinctively, W_6 only contains W–O–W(1); XW_{12} anions feature W–O–W(1) and W–O–W(2); W_{10} contains two distinct W–O–W(1) sites and W–O–W(3) oxygen, whereas P_2W_{18} has three types. The terminal W=O oxo sites are common to all structures. We carried out model protonations at all possible distinct oxygens in each structure. Theses calculations are quite computationally demanding, particularly for the protonated anions, because protonation removes almost all symmetry elements. The calculations for the protonated forms were done under the restrictions of the C_s group symmetry with the exception of the structures corresponding to the protonation at W–O–W(2) in the Keggin and Dawson anions, which were computed with C_1 symmetry. For the protonations at $W_6O_{19}^{2-}$ we verified that the protonation energies almost not change if the calculations are performed without symmetry restrictions (less than 0.5 kcal mol^{-1} for the absolute values and less than 0.1 kcal for the relative protonation energies).

Table 1 contains a list of PEs for some single-addenda polyoxotungstates. Protonations at W=O are in all cases less exothermic than at any W–O–W, irrespective of the anion considered [18]. In general, the basicity of the bridging sites increases in the order: W–O–W(3) < W–O–W(2) < W–O–W(1), a fact which correlates with the ∠W–O–W angle, namely, 163–175°, 150–152° and 117–128°, respectively. It has been previously suggested that the acid strength of a bridging site is affected by a number of factors including the bond angle of the W–O–W triad [19].
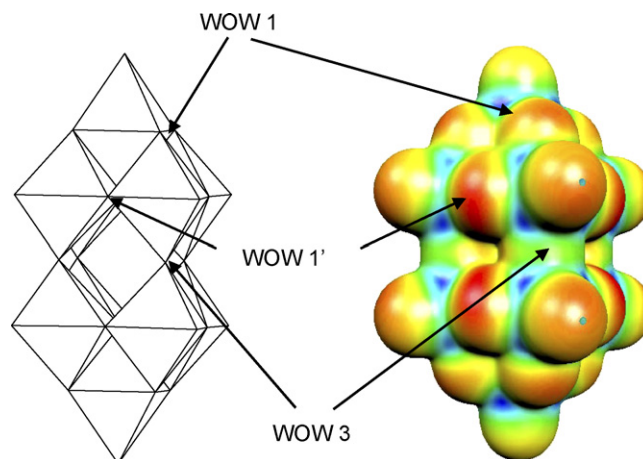

Fig. 2. Molecular electrostatic potential (MEP) for decatungstate. Red identifies more nucleophilic regions and green and blue denotes regions less nucleophilic. (For interpretation of the references to color in this figure legend, the reader is referred to the web version of the article.)

From the theoretical point of view, the topology of the molecular electrostatic potentials (MEP) has proved to be useful for detecting the most nucleophilic regions of a POM [20]. Electrophilic species tend to minimize their potential energy by approaching as much as possible a minimum of the MEP distribution. Fig. 2 shows the computed MEP for $W_{10}O_{32}^{4-}$, where red identifies regions in which the electrostatic potential is negative (nucleophilic regions) and blue regions with a less negative potential (more electrophilic regions). This MEP distribution clearly shows that the equatorial bridging oxygens, W–O–W(3), which link the two W_5 moieties, are less nucleophilic than the other two bridging sites. The calculations carried out for the protonated cluster corraborate the qualitative picture given by the MEP distribution. The PE computed for W–O–W(3) is 3.6 and 9.5 kcal mol^{-1} less negative than for W–O–W(1) and W–O–W(1′), respectively.

The effect of the molecular charge is also notable since, for Keggin clusters for example, each additional unit charge makes protonations 3–5 kcal mol^{-1} more exothermic for all the sites considered. The P_2W_{18} cluster possesses the largest total charge ($q = −6$) of the series and consequently, all sites present quite
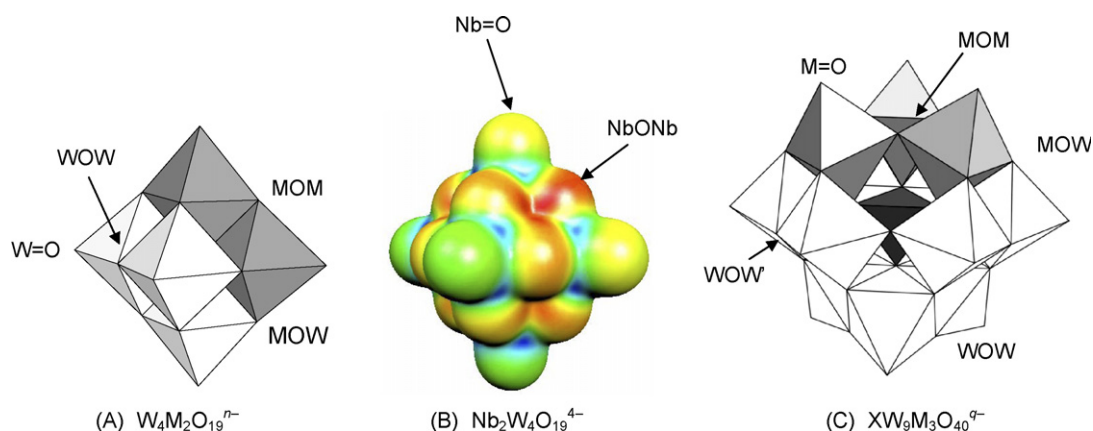

Fig. 3. Polyhedral view and oxygen labeling for Lindqvist (A) and mixed-addenda Keggin (C) anions, and MEP distribution for $Nb_2W_4O_{19}^{4-}$ (B). White and grey polyhedra are W- and M-centered, respectively. The color coding for the MEP distribution is equivalent to that of Fig. 2.

Table 2
Computed energies at different protonation sites for the $[W_4M_2O_{19}]^{q-}$ + $H_3O^+ \rightarrow [HM_2W_4O_{19}]^{(q-1)-} + H_2O$ reactions for M=Nb, V, Ta and Ti[a]

M	WOW	MOW	MOM	M=O	W=O
W	0.00	–	–	–	+7.6
Nb	−16.0	−16.8	−18.8	−15.1	−6.1
V	−14.8	−17.7	−14.9	−6.1	−9.7
Ta	−14.7	−15.5	−17.9	−18.9	−4.6
Ti	−30.5	−30.0	−36.2	−34.2	−18.6

[a] Values are in kcal mol^{-1}.

Table 3
Protonation energies at different sites for $[W_{6-x}Nb_xO_{19}]^{(2+x)-}$, $x = 1$–6[a]

x	NbONb	Nb=O	NbOW	WOW	W=O
1	–	−9.8	−9.8	−8.4	−2.5
2	−18.7	−15.1	−16.8	−16.0	−6.1
3	−25.8	−21.9	−24.6	−27.8	−11.0
4	−29.7	−26.4	−28.7	−28.7	−17.1
5	−37.1	−33.1	−42.5	–	−23.1
6	−46.5	−43.6			

[a] Values are in kcal mol^{-1}.

large PEs. The most basic site is the W–O–W(1) oxygen, and the least, the terminal W=O, but the difference between these two sites is smaller than for the other single-addenda anions. Although we do not report the data here, we also computed the PEs for several Keggin molybdates. As reported previously by other authors, the molybdates were systematically found to be more basic than the homologous tungstates [8,21].

3.2. Mixed-addenda compounds

In this section, we analyze the results for $W_{6-x}M_xO_{19}{}^{q-}$ and $XW_9M_3O_{40}{}^{q-}$ anions. Fig. 3 shows some of the structures discussed. The reader may notice that the XW_9M_3 clusters studied have MO_6 units that share corners, since it is the most common form for threefold-substituted Keggin anions [22]. The twofold- and fourfold-substituted Lindqvist clusters have two positional isomers each: the *cis* structure, with C_{2v} symmetry, and the *trans* form, with D_{4h} symmetry. The former was found to be slightly more stable than the *trans* isomer in the present work, as in other papers reported to date [23,24]. Consequently, the $W_2M_4O_{19}$ and $W_4M_2O_{19}$ forms discussed below are of the *cis* type. Although there are two isomeric forms of the $W_3M_3O_{19}$ clusters, we computed only the *mer* structure; the possible energy difference existing between them would not affect the general trends arising from this work. In clusters of the $W_6O_{19}{}^{2-}$ family, the central O^{2-} atom can be viewed as an isolated entity, accommodating almost the entire negative charge of the cluster [1,6,25]. Many of the mixed-addenda derivatives of the hexatungstate have been investigated in deep by Klemperer and co-workers [26]. Keggin and Dawson structures can also be described using the clathrate model; for example: $PO_4{}^{3-}$ at $W_{12}O_{36}$ or $\{PO_4{}^{3-}\}_2$ at $W_{18}O_{58}$ [9].

3.2.1. Mixed-addenda Lindqvist anions

The anions investigated are $W_{6-x}M_xO_{19}{}^{q-}$ with M = Ta^V, Nb^V, V^V, and Ti^{IV}. The number of distinct protonation sites depends on the substitution degree, x. Fig. 3 shows the five oxygen types for which the isomers $HW_4M_2O_{19}{}^{+1-q}$ were computed. All the protonated structures (Lindqvist and Keggin) were optimized under the restrictions of the C_s group symmetry.

Let us start the analysis of the mixed M/W clusters with the disubstituted anion $W_4M_2O_{19}{}^{q-}$. The energies involved in the protonation at W–O–W, M–O–W, M–O–M, M=O and W=O are given in Table 2. A simple analysis of the MEP distribution of the Nb derivative (Fig. 3B) indicates that the substituted region should be the most favorable for a protonation and that the ter-

minal W=O oxygen is not a good position for protonation. The red area in the domains of Nb–O–Nb oxygens is a strong signal that the nucleophilicity of these sites will be large. The PE values in Table 2 confirm the qualitative predictions made from the MEP distributions; for $W_4Nb_2O_{19}{}^{4-}$, the preferred site for protonation is Nb–O–Nb, but we can observe that the differences in the PEs among the three bridging oxygens are modest, the W–O–W oxygen being the least basic. When M is Ti, protonation shall also occur at the disubstituted bridging site, Ti–O–Ti. The case of $W_4V_2O_{19}{}^{4-}$ seems somewhat anomalous. We also expected the V–O–V to be the most basic, but we computed PE to be larger for W–O–V. In vacuum these two sites were found degenerate.

In this series of Lindqvist anions the computed PEs were moderately different at constant anion charge: that is, all protonations at W–O–W, M–O–W or M–O–M are similar, irrespective of M. Larger differences appear in the nucleophilicity of terminal M=O oxygens, though. For the isoelectronic $W_4M_2O_{19}{}^{4-}$ anions (M=Nb, V and Ta), we computed PEs at M=O of −15.1, −6.1 and −18.9 kcal mol^{-1}, respectively. This may indicate that the basicity of the M=O sites is much more dependent on M than the basicity at bridging sites. Evidently, protonation at Ti=O is, by far, the most exothermic process for two reasons: the higher negative charge of the anion and the presumed lowest Ti=O bond strength [27]. On the other hand, in vanadium-containing clusters, the V=O terminals are much less basic than bridging sites and other M^V=O moieties (see Table 2). This may also be explained by the V=O bond strength [28], which is similar to that of W=O. As expected, the nucleophilicity of W=O moieties is always low.

In $W_{6-x}M_xO_{19}{}^{q-}$ anions, the only variables that affect the basicity are the nature of M and the molecular charge (associated to the degree of substitution, x). For Nb^V, V^V and Ti^{IV}, each new substitution brings an additional negative charge to the cluster. In Table 3, we show the dependence between the PE and the total molecular charge of the cluster for the $[W_{6-x}Nb_xO_{19}]^{(2+x)-}$ series.

The PEs of all the substituted clusters are invariably more negative than those of $W_6O_{19}{}^{2-}$. Values for Nb–O–Nb, Nb=O and W=O in Table 3 are represented graphically in Fig. 4 versus the total molecular charge, q. The reader may observe that larger q values increase the nucleophilicity of the anions for the all sites considered. In general, when the total molecular charge increases by one unit, the protonation energy becomes 6.7, 6.6 and 5.2 kcal mol^{-1} more negative for Nb–O–Nb, Nb=O and W=O sites, respectively. For $x = 4$ ($q = -6$), the PE for Nb–O–Nb

Table 4

Relative protonation energies (PE) computed at different oxygen sites for $[X^{n+}W_9M_3O_{40}]^{q-}$ (M=V, Nb and Ti), with $n = 3$, 4 and 5[a]

M	X	q	M=O	MOM	MOW	WOW	WO'W	W=O	PE$_{av}$[b]	ΔPE[b]
V	Al	8	−21.0	−24.3	−21.6	−20.1	−18.3	−12.0	−19.6	12.3
	Si	7	−13.7	−21.7	−17.7	−14.9	−17.6	−6.2	−15.3	15.5
	P	6	−6.6	−18.7	−13.5	−10.1	−7.9	−0.4	−9.5	18.3
Nb	Al	8	−22.9	−22.2	−19.0	−21.3	−19.1	−10.1	−19.1	12.8
	Si	7	−17.4	−18.8	−14.2	−14.6	−13.6	−4.5	−13.9	14.3
	P	6	−13.5	−16.2	−10.7	−9.6	−10.2	−0.2	−10.1	16.0
Ti[b]	Al	11	−48.8	−45.6	−33.2	−33.2	−26.6	–	–	–
	Si	10	−41.9	−44.8	−31.1	−26.2	−23.7	−19.3	−30.5	29.8
	P	9	−35.4	−38.3	−23.6	−19.8	−15.9	−9.5	−23.8	26.3

[a] Values, relative to protonation of W_6O_{19}, are in kcal mol^{-1}; PE$_{av}$ is the average of the five protonation energies and ΔPE is the difference between the largest and smallest PE.

[b] The isomer HAlW$_9$Ti$_3$ with the proton attached at W=O did not converged and the corresponding PE was not computed.
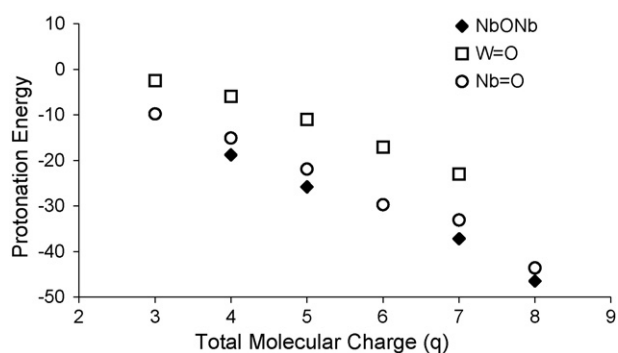

Fig. 4. Protonation energies at Nb–O–Nb, Nb=O and W=O sites (in kcal mol^{-1}) vs. q, for $[W_{6-x}Nb_xO_{19}]^{q-}$. The reference zero-energy corresponds to the protonation at the W–O–W site in the single-addenda $W_6O_{19}^{2-}$ anion.

is somewhat less negative than expected. The dependence found is close to linearity only with regard to the total molecular charge and the protonation site. We also studied this behavior for the same series of clusters with M=V and Ti but observed no significant differences.

3.2.2. Mixed-addenda Keggin anions

The effect of metal substitution was also studied in Keggin anions. PEs at different oxygen sites for XW$_9$M$_3$O$_{40}$$^{q-}$ (with X = P^V, Si^{IV}, Al^{III} and M=V^V, Nb^V, Ti^{IV}) are given in Table 4. Unlike the Lindqvist anions, the substituted region is significantly more basic than the unsubstituted one. In PW$_9$V$_3$O$_{40}$$^{6-}$, for example, the most basic site is the bridging oxygen bonded to two V^V ions, with relative PE of −18.7 kcal mol^{-1}. The bridging oxygen linked to a W^{VI} and V^V is the second most basic site with a PE of −13.5 kcal mol^{-1} and the two W–O–W sites studied have smaller PEs of −10.1 and −7.9 kcal mol^{-1}, respectively. As expected, the least basic sites are the terminal oxygens linked to W^{VI}, with protonation energies of about +18 kcal mol^{-1} in relation to V–O–V. The V=O site also has a low proton affinity (PE = −6.6 kcal mol^{-1}). Interestingly, the relative energies in silicates and aluminates present some differences from those in phosphates. The values in Table 4 show that increasing the negative charge equalizes somewhat the basicity of all sites. Hence, the difference in the PE between the most (V–O–V) and

least (W=O) basic sites decreases from +18.3 kcal mol^{-1} in the phosphate ($q = -6$) to 15.5 kcal mol^{-1} in the silicate ($q = -7$) and is as high as +12.3 kcal mol^{-1} in the aluminate ($q = -8$). It is also noteworthy that the difference in basicity between the V–O–V and V=O sites depends very much on X. In PW$_9$V$_3$O$_{40}$, the protonation at V=O is very unfavorable, +12.1 kcal mol^{-1} less than V–O–V but, in AlW$_9$V$_3$O$_{40}$, the difference is only +3.3 kcal mol^{-1}. This behavior can be rationalized if it is taken into account that the oxygen bonded to Al (in the central AlO$_4$ unit) is a more electron donating trans ligand (trans to the V=O bond) than the O atom from PO$_4$. Consequently, the V=O distance increases from X = P (1.626 Å) to Al (1.642 Å) in the same way as the negative charge on the terminal V=O oxygen also does (Table 5).

The substitution of three W^{VI} by three Nb^V in PW$_{12}$ has more or less the same effect as the substitution by V^V. That is, after substitution the substituted region becomes the most basic, the bridging substituted site Nb–O–Nb being the most easily protonated. As usual, W=O is the least basic site with a relative protonation energy of 16.0 kcal mol^{-1} in relation to Nb–O–Nb; the corresponding value for PW$_9$V$_3$ is +18 kcal mol^{-1}. PEs at V–O–V are, systematically, more negative than the homologous Nb-sites. In contrast, PEs are greater for Nb=O than for V=O by about 4–7 kcal mol^{-1}. This is probably related to the higher negative charge on the terminal oxygen when it is bonded to Nb (Table 5) and to the stronger V=O bonds [28]. Notice that in AlW$_9$Nb$_3$ the Nb=O site is actually the most basic site with protonation energy of −22.9 kcal mol^{-1}.

Table 5

M=O distances and net charges on terminal M=O oxygens for several XW$_9$M$_3$O$_{40}$$^{q-}$ anions[a]

X	M=V		M=Nb		M=Ti	
	d$_{M=O}$	Q (O)	d$_{M=O}$	Q (O)	d$_{M=O}$	Q (O)
P	1.626	−0.709	1.773	−0.896	1.726	−0.857
Si	1.636	−0.719	1.783	−0.919	1.735	−0.880
Al	1.642	−0.759	1.795	−0.937	1.742	−0.903

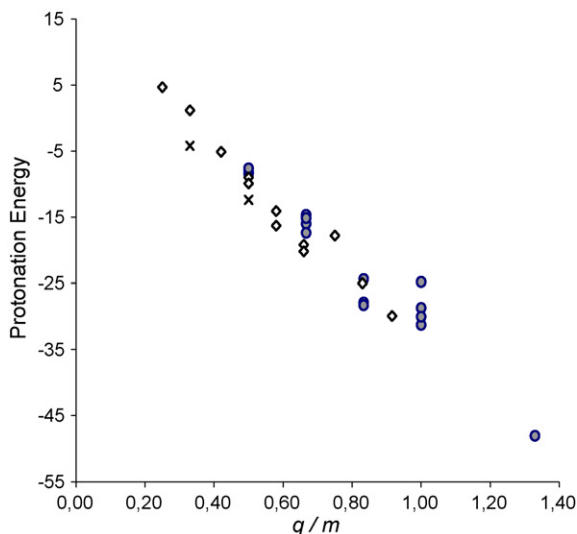[a] Distances in Å. Net charges were obtained from Mulliken population analysis.

Fig. 5. Computed protonation energies (in kcal mol^{-1}) for some POM architectures at bridging W–O–W oxygens, represented vs. their q/m ratios. Diamonds, circles and crosses represent Keggin, Lindqvist, and Dawson anions, respectively. All the protonation energies are referred to the protonation W–O–W site in $W_6O_{19}^{2-}$.

The case of titanates clearly shows the effect of the lower oxidation state of Ti^{IV}, which causes its derivatives to be more negatively charged. Therefore, the PEs computed are by far the most negative. Ti^{IV} ions induce larger polarizations than pentavalent ions in the anion skeleton and, consequently, the difference between the basicity of substituted and unsubstituted regions is larger in titanates than in vanadates or niobates. The values of ΔPE in Table 4 clearly show this. Hence, the bridging Ti–O–Ti oxygen and the terminal Ti=O are significantly more nucleophilic than all the other sites. It is also significant that Ti=O is much more basic than Ti–O–W, which means that in monosubstituted tungstotitanates the proton will always attach the terminal Ti=O oxygen. In the titanates studied, the basicity of the terminal Ti=O oxygen again becomes more basic than the other sites when going from X = P^V to X = Al^{III}.

3.3. The effect of charge and size on the basicity of the clusters

In the sections above, we have shown that when the cluster charge increases, the anion becomes significantly more basic. It is also easily understandable that the effect of the charge depends on the size of the cluster. Increasing the charge by one unit in a large cluster is much less important than in a small cluster. If we want to compare the effect of the charge in different architectures, the charge must be normalized. In a previous paper [29], we showed that some redox properties can be rationalized with the help of a pseudo-charge density defined as q/m, where q is the charge of the anion and m is the number of metal ions. This latter variable emulates the size of the cluster. Fig. 5 shows the PE at the W–O–W site versus the q/m ratio for several unsubstituted and mixed anions containing Lindqvist, Keggin and Dawson architectures. The figure clearly shows that there is a more or less linear dependence between the protonation energy

at the W–O–W site and the q/m ratio. The q/m values are largest in the most charged Lindqvist clusters. The trisubstituted titanium Lindqvist clusters ($q/m = 1$) are very basic anions. Clusters with associated values of q/m larger than 1 are quite uncommon. Notice, for example, that many giant structures support very large negative charges [30], but in general, the ratio q/m is much smaller than 1. In the opposite site, $PW_{12}O_{40}^{3-}$ has quite a small value of q/m (0.25) and is an anion with low basicity. The absence of a perfect correlation between q/m and PE suggests that other factors besides the pseudo-charge density may affect the nucleophilicity of a given site: for example, the relative distance of the site from the substituted center, the more or less large polarization of the molecule, the bonding angle, etc.

4. Conclusions

Present density-functional calculations carried out for a series of polyoxometalates show that the protonation energy of a given oxygen site depends on various factors. Roughly, in order of importance, they are the number and nature of metal centers directly bonded to an oxygen site, the charge of the anion, and the bonding angle in the bridging oxygen sites In single-addenda anions, protons are preferentially attached to the bridging oxygen with the smallest bonding angle.

When a W^{VI} is substituted by a metal with a lower oxidation state, the charge of the anion increases and therefore the overall basicity of the polyoxometalate also does, where the nucleophilicity of the substituted region is significantly greater. The polarization induced by metal substitution is more important in the larger Keggin anions than in the Lindqvist anions. In mixed-addenda Keggin anions, the nucleophilicity of the terminal M=O oxygens was found to be very sensitive to the nature of the central cation, X, because of the trans effect of the oxygen bonded to X in the central XO_4 fragment.

The total charge of the anion is very important but its effect depends on the cluster size. For the same site type (W–O–W), we have found that the PE energy depends more or less linearly on the ratio q/m, where q is the charge of the anion and m is the number of metal ions. This latter variable emulates the size of the cluster and q/m may be considered as a pseudo-charge density.

References

[1] M.T. Pope, Heteropoly and Isopoly Oxometalates, Springer-Verlag, Berlin, 1983.
[2] J.J. Borrás-Almenar, E. Coronado, A. Müller, M.T. Pope, Polyoxometalate Molecular Science, Kluwer Academic Publishers, Dordrecht, 2003.
[3] I.V. Kozhevnikov (Ed.), Catalysis by Polyoxometalates, John Wiley & Sons, Chichester, 2002.
[4] C. Tourné, G. Tourné, Bull. Soc. Chim. Fr. (1969) 11244.

[5] See, for example;
(a) D.C. Duncan, R.C. Chambers, E. Hecht, C.L. Hill, J. Am. Chem. Soc. 117 (1995) 681, and references therein;
(b) F. Cavani, M. Koutyrev, F. Trifirò, Catal. Today 28 (1996) 319;
(c) V. Kogan, Z. Aizenshtat, R. Neumann, Angew. Chem. Int. Ed. 38 (1999) 3331;
(d) A. Bagno, M. Bonchio, A. Sartorel, G. Scorrano, Eur. J. Inorg. Chem. (2000) 17;
(e) O.A. Kholdeeva, G.M. Maksimov, R.I. Maksimovskaya, L.A. Kovaleva, M.A. Fedotov, V.A. Grigoriev, C.L. Hill, Inorg. Chem. 39 (2000) 3828;
(f) H. Zeng, G.R. Newkome, C.L. Hill, Angew. Chem. Int. Ed. 39 (2000) 1771, and ref. [2] therein;
(g) A.M. Khenkin, L.J. Shimon, R. Neumann, Eur. J. Inorg. Chem. (2001) 789;
(h) Y. Nishiyama, Y. Nakagawa, N. Mizuno, Angew. Chem. Int. Ed. 40 (2001) 3639;
(i) A. Troupis, A. Hiskia, E. Papaconstantinou, Angew. Chem. Int. Ed. 41 (2002) 1911;
(j) R. Ben-Dabiel, R. Neumann, Angew. Chem. Int. Ed. 42 (2003) 92;
(k) V. Mirkhani, S. Tangestaninejad, B. Yadollahi, L. Alipanah, Catal. Lett. 91 (2003) 129;
(l) K. Kamata, K. Yonehara, Y. Sumida, K. Yamaguchi, S. Hikichi, N. Mizuno, Science 300 (2003) 964;
(m) S.P. Maradur, S.B. Halligudi, G.S. Gokavi, Catal. Lett. 96 (2004) 165;
(n) O.A. Kholdeeva, M.P. Vanina, M.N. Timofeeva, R.I. Maksimovskaya, T.A. Trubitsina, M.S. Melgunov, E.B. Burgina, J. Mrowiec-Bialon, A.B. Jarzebski, C.L. Hill, J. Catal. 226 (2004) 363;
(o) W.B. Kim, T. Voitl, G.J. Rodriguez-Rivera, J.A. Dumesic, Science 305 (2003) 1280.
[6] V.W. Day, W.G. Klemperer, Science 228 (1985) 533.
[7] M.T. Pope, E. Papaconstantinou, Inorg. Chem. 6 (1967) 237.
[8] T. Okuhara, N. Mizuno, M. Misono, Adv. Catal. 41 (1996) 113.
[9] J.M. Poblet, X. López, C. Bo, Chem. Soc. Rev. 32 (2003) 297.
[10] ADF 2003.01, Department of Theoretical Chemistry, Vrije Universiteit, Amsterdam. E.J. Baerends, D.E. Ellis, P. Ros, Chem. Phys. 2 (1973) 41;
L. Versluis, T.J. Ziegler, Chem. Phys. 88 (1988) 322;
G. Te Velde, E.J. Baerends, J. Comput. Phys. 99 (1992) 84;
C. Fonseca Guerra, J.G. Snijders, G. Te Velde, E.J. Baerends, Theor. Chem. Acc. 99 (1998) 391.
[11] A.D. Becke, J. Chem. Phys. 84 (1986) 4524;
A.D. Becke, Phys. Rev. A38 (1988) 3098.
[12] S.H. Vosko, L. Wilk, M. Nusair, Can. J. Phys. 58 (1980) 1200.
[13] J.P. Perdew, Phys. Rev. B33 (1986) 8822;
J.P. Perdew, Phys. Rev. B34 (1986) 7406.
[14] A. Klamt, G.J. Schüürmann, Chem. Soc. Perkin Trans. 2 (1993) 799;
J. Andzelm, C. Kölmel, A.J. Klamt, Chem. Phys. 103 (1995) 9312;
A.J. Klamt, Chem. Phys. 99 (1995) 2224.
[15] C.C. Pye, T. Ziegler, Theor. Chem. Acc. 101 (1999) 396.
[16] We will employ the commonly used shorthand notation for polyoxometalate molecular formulas, in which neither oxygens nor charge are specified (i.e., W_6 for $W_6O_{19}{}^{2-}$ or SiW_{12} for $SiW_{12}O_{40}{}^{4-}$).
[17] X. López, J.A. Fernández, S. Romo, J.F. Paul, L. Kazansky, J.M. Poblet, J. Comput. Chem. 25 (2004) 1541.

[18] From the experimental point of view, this is still an unclear question given that several reports addressed on this topic point, apparently, to different directions. See:
J.B. Moffat, J. Mol. Catal. 26 (1984) 385;
J.N. Barrows, G.B. Jameson, M.T. Pope, J. Am. Chem. Soc. 107 (1985) 1771;
K.Y. Lee, N. Mizuno, T. Okuhara, M. Misono, Bull. Chem. Soc. Jpn. 62 (1989) 1731;
I.V. Kozhevnikov, Russ. Chem. Rev. 56 (1987) 1417;
I.V. Kozhevnikov, Catal. Lett. 34 (1995) 213.
[19] N.O. Gonzales, A.K. Chakraborty, A.T. Bell, Catal. Lett. 50 (1998) 135.
[20] (a) J.Y. Kempf, M.-M. Rohmer, J.M. Poblet, C.M.J. Bénard, J. Am. Chem. Soc. 114 (1992) 1136;
(b) X. López, C. Bo, J.M. Poblet, J. Am. Chem. Soc. 124 (2002) 12574.
[21] (a) B.B. Bardin, S.V. Bordawekar, M. Neurock, R.J. Davis, J. Phys. Chem. B 102 (1998) 10817;
(b) B.B. Bardin, R.J. Davis, M. Neurock, J. Phys. Chem. B 104 (2000) 3556.
[22] E. Cadot, R. Thouvenot, A. Tézé, G. Hervé, Inorg. Chem. 31 (1992) 4128.
[23] J.M. Maestre, J.P. Sarasa, C. Bo, J.M. Poblet, Inorg. Chem. 37 (1998) 3071.
[24] C. Rocchiccioli-Deltcheff, R. Thouvenot, M. Daddabi, Spectrochim. Acta 33A (1977) 143.
[25] J.M. Maestre, X. López, C. Bo, N. Casañ-Pastor, J.M. Poblet, J. Am. Chem. Soc. 124 (2001) 3749.
[26] (a) W.G. Klemperer, W. Shum, Am. Chem. Soc. 99 (1977) 3544;
(b) W.G. Klemperer, W.J. Shum, Am. Chem. Soc. 100 (1978) 4891;
(c) M. Filowitz, R.K.C. Ho, W.G. Klemperer, Inorg. Chem. 18 (1979) 93;
(d) C.J. Besecker, W.G. Klemperer, J. Am. Chem. Soc. 102 (1980) 7598–7600;
(e) V.W. Day, M.F. Fredrich, M.R. Thompson, W.G. Klemperer, R.S. Liu, W. Shum, J. Am. Chem. Soc. 103 (1981) 3597;
(f) C.J. Besecker, W.G. Klemperer, V.W. Day, J. Am. Chem. Soc. 104 (1982) 6158;
(g) C.J. Besecker, V.W. Day, W.G. Klemperer, M.R. Thompson, J. Am. Chem. Soc. 106 (1984) 4125;
(h) V.W. Day, W.G. Klemperer, D. Maltbie, J. Organometall. 4 (1985) 104;
(i) C.J. Besecker, V.W. Day, W.G. Klemperer, M.R. Thompson, Inorg. Chem. 24 (1985) 44;
(j) V.W. Day, W.G. Klemperer, C. Schwartz, J. Am. Chem. Soc. 109 (1987) 6030;
(k) V.W. Day, W.G. Klemperer, D.J. Maltbie, J. Am. Chem. Soc. 109 (1987) 2991;
(l) V.W. Day, W.G. Klemperer, S.P. Lockledge, D. Main, J. Am. Chem. Soc. 112 (1990) 2031;
(m) V.W. Day, W.G. Klemperer, D. Main, J. Inorg. Chem. 29 (1990) 2345;
(n) V.W. Day, W.G. Klemperer, D. Main, J. Inorg. Chem. 29 (1990) 2355.
[27] H.J. Kim, S.-H. Byeon, H. Yun, Bull. Korean Chem. Soc. 22 (2001) 298.
[28] O. Dmitrenko, W. Huang, T.E. Polenova, L.C. Francesconi, J.A. Wingrave, A.V. Teplyakov, J. Phys. Chem. B 107 (2003) 7747.
[29] X. López, J.A. Fernández, J.M. Poblet, Dalton Trans. (2006) 1162.
[30] E.T.K. Haupt, C. Wontorra, D. Rehder, A. Müller, Chem. Commun. (2005) 3912;
A. Müller, E. Beckmann, H. Bögge, M. Schmidtmann, A. Dress, Angew. Chem. Int. Ed. 41 (2002) 1162;
A. Müller, F. Peters, M.T. Pope, D. Gatteschi, Chem. Rev. 98 (1998) 239.